# NATURAL VARIATIONS IN THE GEOMAGNETICALLY TRAPPED ELECTRON POPULATION

A. L. VAMPOLA
Space Physics Laboratory
The Aerospace Corporation
El Segundo, California

## ABSTRACT

Temporal variations in the trapped natural electron flux intensities and energy spectra are discussed and demonstrated using recent satellite data. These data are intended to aquaint the space systems engineer with the types of natural variations that may be encountered during a mission and to augment the models of the electron environment currently being used in space system design and orbit selection (i.e., AE3 by Vette et al., refs. 2 and 3). These models, while excellent in some respects and quite satisfactory in most other respects, were generated before high resolution spectrometry data were generally available. For systems or subsystems which are particularly sensitive to radiation and respond to changes in the environment on a short time scale, these models by themselves may be inadequate for proper subsystem design or interpretation of on-orbit data. An understanding of the temporal variations which may be encountered should prove helpful. Some of the variations demonstrated here which are not widely known include: addition of very energetic electrons ($E \geq 5$ MeV) to the outer zone during moderate magnetic storms; addition of energetic electrons ($E > 1$ MeV) to the inner zone during major magnetic storms; inversions in the outer zone electron energy spectrum during the decay phase of a storm injection event; occasional formation of multiple maxima ($\geq 4$) in the flux vs altitude profile of moderately energetic electrons ($E \leq 1$ MeV).

---

This work was conducted under U. S. Air Force Space and Missile Systems Organization (SAMSO) Contract No. F04701-70-C-0059.

In the design of spacecraft systems, subsystems, and sensors, a knowledge of the radiation environment which will be encountered is essential. In the case of a particularly vulnerable sensor or biological subsystem, the configuration of the trapped radiation belts may even be a major factor in the choice of orbit. Excellent models of the average environment are available (refs. 1 and 2) but have limitations, especially their treatment of short-term spectra effects. More data are now available on what could be called "second-order" effects, and will be treated here, since for particularly vulnerable or sensitive payloads a knowledge of these "second-order" effects may be a prerequisite for proper design, functioning, or data analysis. Since we are considering short-term fluctuations in the trapped particle environment from the point of view of obtaining better criteria for system design and orbit selection, magnetospheric physics will not be emphasized here. This is perhaps just as well, since the physical processes involved in the formation of the belts are not well understood and are only indirectly relevant to our goal -- it is the final result of these processes, the radiation environment, which is used as an input to space system design.

The geomagnetically trapped natural electrons fall into two primary classes: a) the inner zone which is relatively stable and exhibits a "soft" electron spectrum (i.e., a steep differential energy spectrum with few energetic particles); and b) the outer zone which is just the converse. Here the flux intensities vary widely on a short time scale and at times the spectrum is quite hard. The outer zone includes the synchronous-orbit environment. Because of the particular importance and high usage of this orbit, the synchronous environment will be treated separately.

## OUTER ZONE AND SLOT VARIATIONS

Measurements of magnetospheric electron fluxes by many investigators have shown large changes in the outer zone electron population in response to magnetic activity. For instance, Frank, in a statistical study of electrons with energies greater than 40 keV (ref. 3), showed the great variability of the total flux in the outer zone and (ref. 4) presented evidence for inward diffusion of electrons with $E > 1.6$ MeV. Williams et al. (ref. 5) showed a correlation between the magnitude of the magnetic activity and the L-value at which peak flux intensities were observed. L is McIlwain's parameter (ref. 6) and for our purposes can be taken as the geocentric radial distance, in units of earth radii, at which a particular magnetic field line crosses the geomagnetic equator. The field line of interest is the guiding center of a geomagnetically trapped particle and under appropriate circumstances can be assumed to remain constant for a particular particle while that particle executes bounce and drift motion.

Williams et al. (ref. 5) also showed that for electrons with $E > 300$ keV, the time for low altitude outer zone electron fluxes to reach equilibrium with equatorial fluxes is $\leq 0.1$ day. We shall utilize this finding and assume that low altitude data is qualitatively and semi-quantitatively representative of the entire outer zone. Most of the data which will be presented was obtained by magnetic spectrometers on two low altitude (apogee $< 6000$ km) elliptical polar orbiting satellites, OV3-3 (1966-70A) and OV1-19 (1969-25C).

Figure 1 shows the effect of a large magnetic storm on energetic electron fluxes at $L = 4$. Unidirectional differential energy fluxes are plotted as a function of time. We see that in addition to a very large change in flux at all energies due to the storm on day 247 (January 1 = day 1), there is a significant effect due to smaller storms on days 278, 290, 302 and perhaps others. The first storm followed a relatively quiet period and hence resulted in a flux increase of about two orders of magnitude. The subsequent storms occurred during the recovery from the first and resulted in smaller relative changes. The high energy electron flux profile was less sensitive to the smaller storms than the low energy flux. Figure 2 shows the effect of the storms in the "slot". Here only the lowest energy electrons exhibit significant effects due to the later storms. However, all show a very large effect due to the day 247 storm -- as much as four orders of magnitude in the 712 keV plot. Note that the onset is very sharp and the decay is relatively fast. Plots of precipitating flux at very low altitude ($\approx$ 400 km) show the primary loss of these particles in the slot is by rapid pitch-angle scattering which lowers the mirror altitude of the particles until

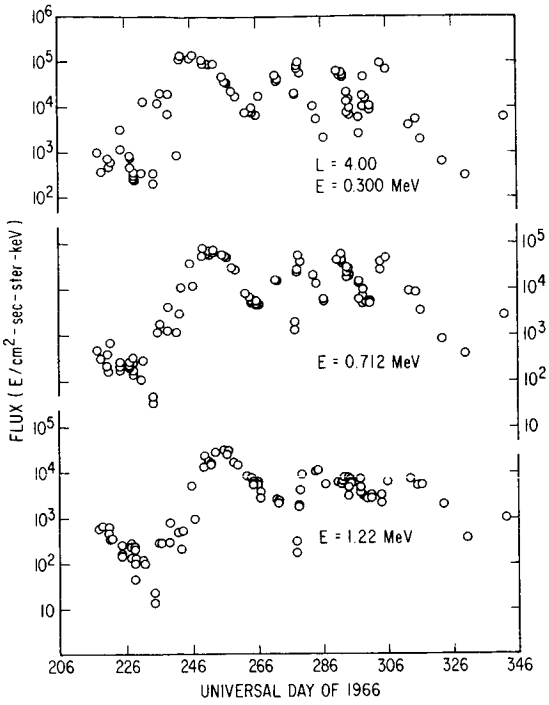


FIGURE 1. -- Electron fluxes at L = 4.0 for 1.225, .712, and .300 MeV during the period day 206 to day 346, 1966. Increases are seen on day 247, 278, 290, and 302 due to magnetic activity.

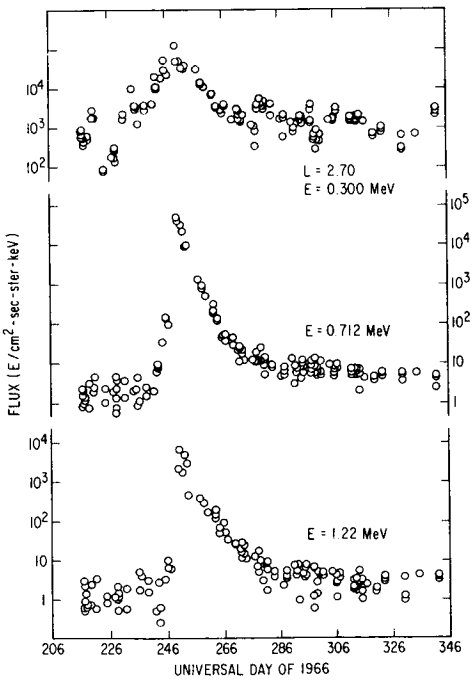


FIGURE 2. -- Electron fluxes at L = 2.7 for 1.225, .712, and .300 MeV during the period day 206 to day 346, 1966. All fluxes show a large increase due to the magnetic storm on day 247, but only the .300 MeV fluxes respond to later minor magnetic disturbances.

they are lost into the atmosphere. Figure 3 shows two examples of electron precipitation -- one with a large flux present in the slot and another with a small flux in the slot, although both exhibit significant outer zone precipitation. There is evidence that there is a continuous precipitation of particles in the outer zone at or outside of the plasmapause. Within the plasmapause, electrons are more stable except for the "slot" region.

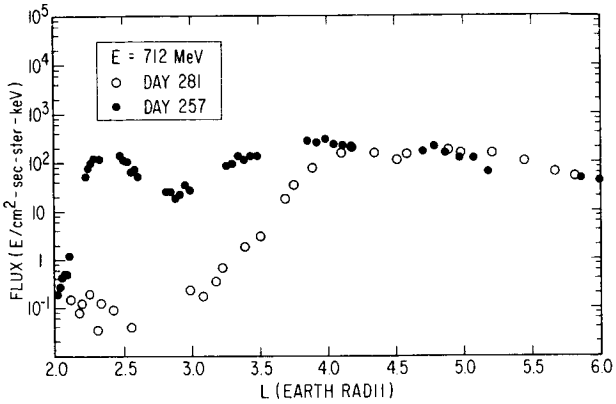


FIGURE 3. -- Low altitude precipitating fluxes for two periods. Significant fluxes are observed in the slot on day 257 but not on day 281. These fluxes are in the drift loss-cone; i.e., they will not survive a complete drift period around the earth.

We can look at the effects of a major magnetic storm from another point of view. For certain purposes, a knowledge of the electron energy spectrum is required. Often measurements are made at a couple of energy thresholds and an exponential or power law spectrum is constructed with those data points. Such a procedure can be hazardous as can be seen from Figures 4 to 6. Flux vs L for a number of electron energies is plotted for several periods preceding and following the large storm on day 247. On day 241 in Figure 4, a large null or "slot" is seen in the flux profile at all energies at $L \approx 3$. The center of the slot appears at slightly higher L values at lower energies. Energy spectra are monotonic almost everywhere. On day 246, the outer zone is much less extensive; solar flare electrons are observed at $L > 6$ and the "slot" is filled with low energy electrons due to minor magnetic disturbances on days 242 and 244. Flux profiles on day 249 show a large peak at $L \approx 3$, the

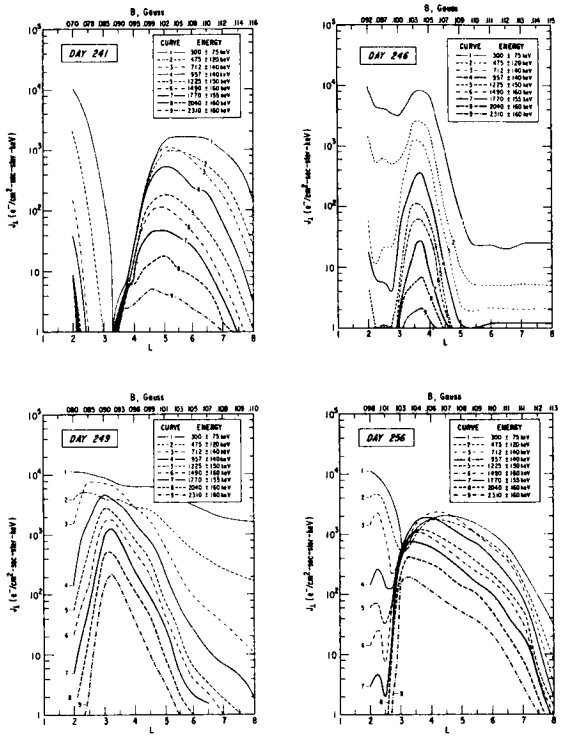


FIGURE 4. -- Plots of $J_1$ (electron flux with a local pitch-angle $\alpha$ = $90^\circ \pm 8^\circ$) vs L for nine differential energy channels for four periods prior to and after the magnetic storm of day 247, 1966. B, the magnetic field in gauss at the point of observation, is annotated for each plot. See text for discussion.

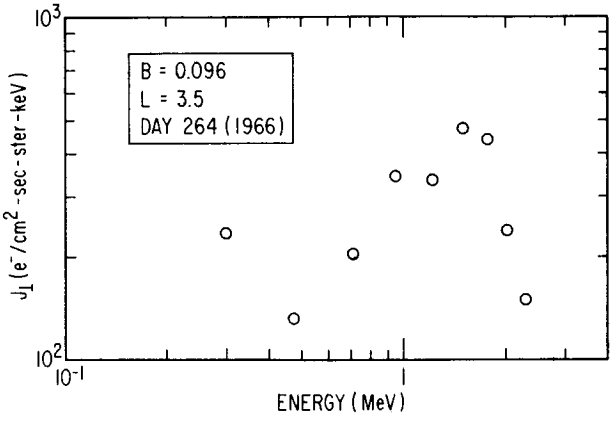


FIGURE 6. -- Differential energy spectrum of electrons at L = 3.5, B = .096 on day 264, 1966. The spectral inversion seen here demonstrates the need for caution in characterizing spectra as exponential or power-law.

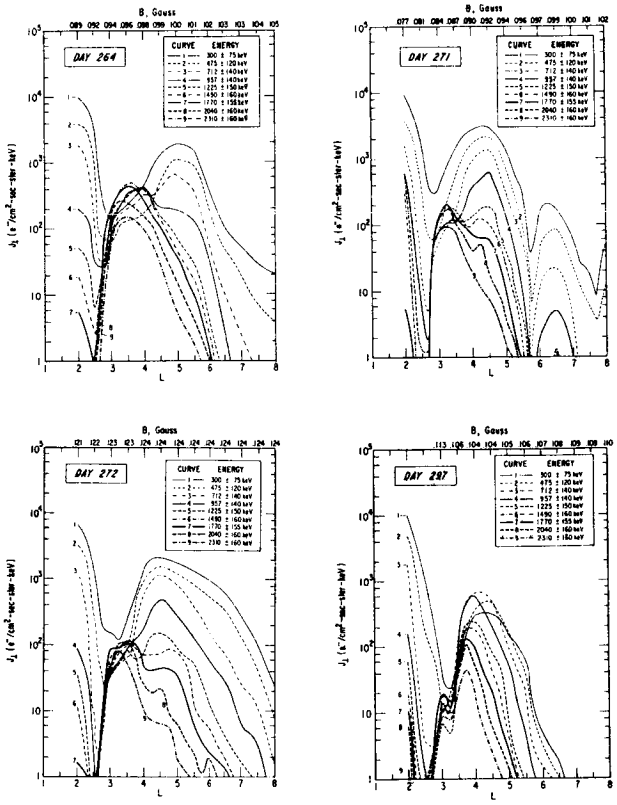


FIGURE 5. -- Plots similar to Figure 4 but for four time periods following those of Figure 4. See text for discussion.

previous location of the slot. The two lowest energy electron flux profiles indicate that some decay may have already taken place. The higher energy fluxes have increased several orders of magnitude from the previous levels. A week later, day 256, the slot is again being established at L ≈ 3. Note that due to the rapid loss there, the profile now has a small peak centered at L ≈ 2.3. Also, note that at L ≈ 3.5, a complex energy spectrum is evolving due to an effective electron lifetime which is longer for the more energetic particles. Figure 5 continues the observations through the next month. On day 264 a rather grotesque energy spectrum has evolved at L = 3.5. This sample spectrum, Figure 6, indicates the need for caution when making flux measurements at one or two energies and extrapolating. The other plots in Figure 5 show other features. On day 271, the outer zone has assumed a multiple-lobed structure. This same structure has been observed in the equatorial fluxes (H. I. West, Jr., private communication) and is probably due to an enhanced localized precipitation producing the minima. It also is possible that the maxima are discrete groups of electrons which have

been injected/accelerated in the outer regions of the outer zone. In fact, since electrons are diffused radially inward and thereby accelerated, both of the above explanations may be correct -- an occasional enhanced precipitation may cause an interruption in an otherwise continuous source of electrons which are being diffused to lower L values. The data of day 272 show that the effects are short-lived and are observable only at lower L values at higher energy, again in agreement with the inward diffusion/acceleration hypothesis. The final plot, day 297, shows a profile qualitatively similar to the initial one on day 241. A small peak near the slot is due to a magnetic disturbance on day 278. In effect, the outer zone has recovered from the large magnetic storm six weeks earlier.

We can observe the effects of magnetic storms on the higher energy particles in Figure 7. These data were obtained from instrumentation on OV1-19 during 1969. A large magnetic storm occurred on May 15. Spectra are shown at L ≈ 3.4 for one week prior to the storm, immediately after the storm, and up to three weeks after the storm. One again sees an evolution of the type seen in the 1966 storm data -- all energy fluxes are enhanced and the subsequent decay is more rapid for the lower energies. Even at 5 MeV significant fluxes of electrons appear. It would be interesting to make detailed measurements at even higher energy during a large storm to see what, if any, is the upper limit to the energy spectrum.

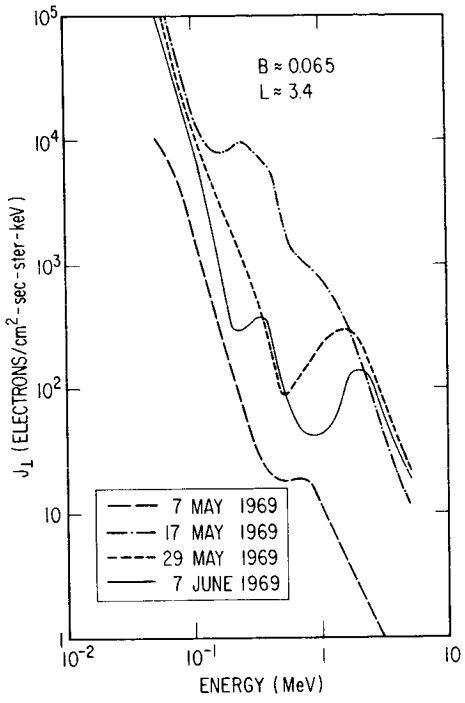


FIGURE 7. -- Energy spectra of electrons between 53 keV and 5.09 MeV at L = 3.4, B = .065 showing the effect of a magnetic storm on 15 May 1969. Significant quantities of electrons between 2 and 5 MeV are injected/accelerated.

## INNER ZONE VARIATIONS

In the inner zone, the information is much less extensive. In the first place, no accurate spectral measurements of natural electrons were made prior to the Starfish nuclear detonation which obscurred the natural population. After that event, any natural flux variation would have had to be very large in absolute value in order to be observed above the artificial addition. Several years were required for the Starfish flux to decay to the point where natural fluxes could be observed. Thus most of the measurements of inner zone electrons in the period 1962 to 1966 were Starfish measurements. Secondly, the inner zone contains a large stable population of very energetic protons and these tend to obscure electron measurements. However, several reports of increases in the inner zone natural electron flux have been made (refs. 7 to 11).

Vampola (ref. 7) compared measurements in 1966 with measurements by Mihalov and White (ref. 12) in 1964 and concluded that the natural electrons in the inner zone had increased by half an order of magnitude in the two year period. Subsequent analysis of data during the 1966 period showed a large change in the inner zone flux during and following the day 247 magnetic storm. Figure 8 is similar to Figures 1 and 2, but shows the effect in the inner zone at L = 1.90. Note that there is an abrupt increase at the time of the storm and then a continuing slight increase for about a month before the fluxes begin to decay. This continuing increase is due to lower energy electrons from higher L values diffusing radially inward and becoming energized. The diffusion rate decreases at lower L values. Hence it takes longer for the fluxes to attain their peak value at lower L values. Figure 9 shows the flux vs L profile for the same time period covered in the outer zone description. The four lowest energy electron profiles show an

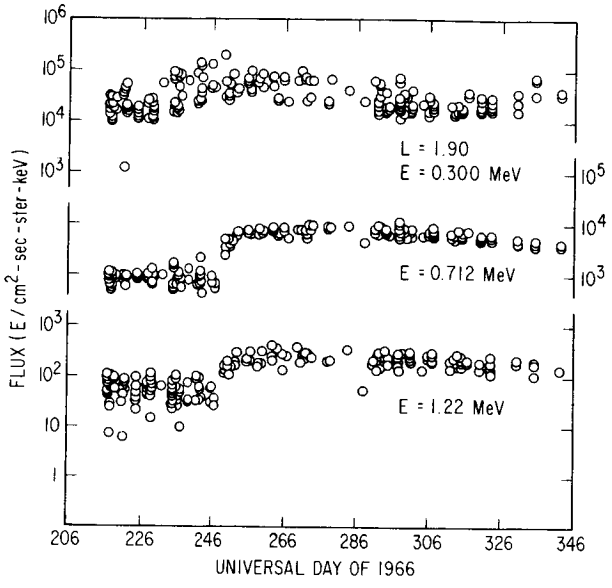


FIGURE 8. -- Plot similar to Figures 1 and 2, but in the inner zone at L = 1.9. The energetic electrons are seen to respond immediately to the magnetic storm on day 247 and then continue to slowly increase in intensity for about a month.

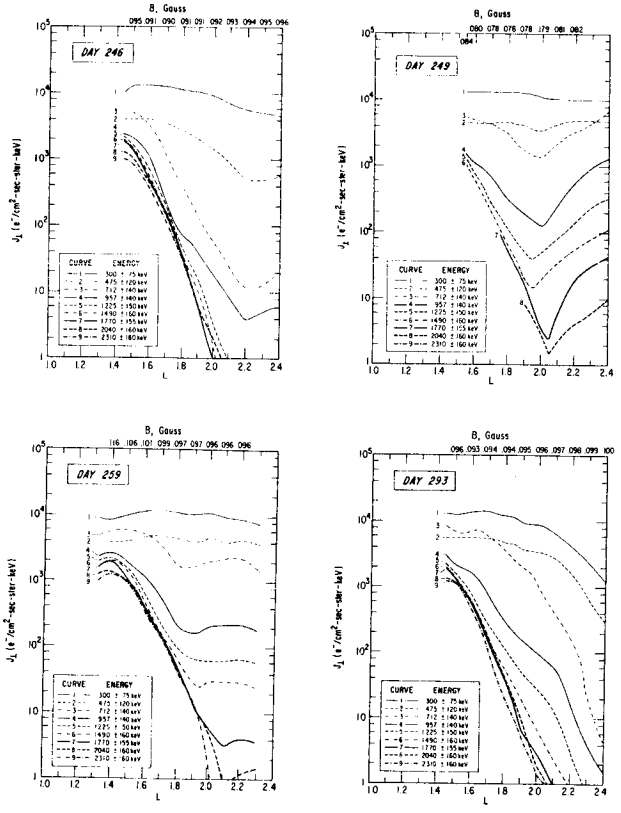


FIGURE 9. -- Plots similar to Figures 4 and 5 but covering the range $1 \leq L \leq 2.4$. Electrons are observed moving to lower L values during the time period covered. See text for discussion.

increase in flux at L ~ 2.2 on day 246. This is due to the small storms which preceded the day 247 storm. Data on day 249 show the large magnetic storm has added electrons of all energies to the inner zone. As these decay away, some also diffuse to lower L values. Data on days 259 and 293 show the evolution of this event. Data on day 293 were taken at approximately the same B (magnetic field) value and are directly comparable. One finds that at L = 1.5, there has been an increase of ≈ 15% in the 957 keV electrons and about 8% in the 1.225 MeV electrons. At L = 1.6, the corresponding figures are about 60% and 15%.

The low energy electrons have been studied extensively by Bostrom et al. (ref. 13) and show pronounced changes due to magnetic activity down to the lower edge of the inner zone. Figure 10 (from ref. 13) presents the time history of $E_e \geq .280$ MeV for L = 1.2, 1.3, 1.5, 1.8, and 2.2 during the period 1963 through 1968. Magnetic storms are indicated by the $D_{st}$ scale. It is seen that the entire inner zone low energy electron population responds to large magnetic storms. Since we are now in the declining phase of solar activity, it can be assumed that the average level of electron flux in the inner zone will decrease. As a result, the perturbations due to magnetic storms will become much more observable.

## VARIATIONS AT SYNCHRONOUS ALTITUDES

Particle detectors at synchronous altitude sample a very small region of B, L space. As a result, it is relatively easy to separate spatial and temporal effects in the electron fluxes observed. There are two principal types of variations -- diurnal and that induced by magnetic activity. During magnetically quiet times, a synchronous satellite will see a slowly varying flux intensity as it samples different local times. Due to the distortion of the magnetosphere, the electron drift shells do not remain at constant radial distance for all local times. The L value at local noon is lower than at local midnight. Since in the region of L = 6.6 (the nominal synchronous L value) the flux intensity decreases with increasing L, a satellite will see smaller fluxes of electrons at local midnight than at local noon. Fig. 11 (from ref. 14) shows this diurnal variation for several energies.

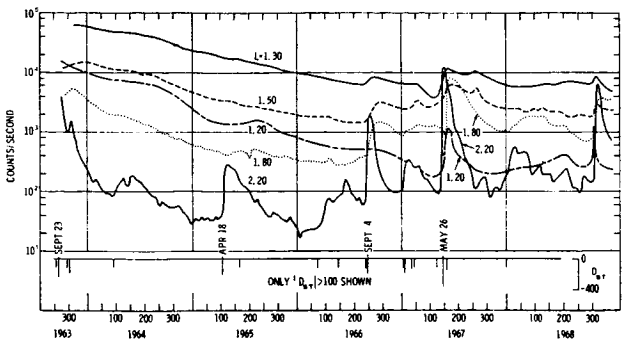


FIGURE 10. -- A history of inner zone low energy electrons ($E_e \geq$ .280 MeV) for L = 1.2, 1.3, 1.5, 1.8, and 2.2. Magnetic storms are indicated by the $D_{st}$ scale, which shows only values of $D_{st} < -100$. The response of these fluxes to magnetic activity is pronounced (from ref. 13).

data was obtained from ATS-1 on 14 January 1967. At approximately 00:08 UT, the magnetometer output shows a reversal of the geomagnetic field. This is interpreted as a motion of the boundary of the magnetosphere past the satellite to a smaller radial distance. Simultaneous with this boundary crossing the particle counters show a loss of flux; at this point they are sampling the interplanetary medium instead of the trapped population in the magnetosphere. A similar situation existed when the data of day 246 (Figure 4) were obtained.

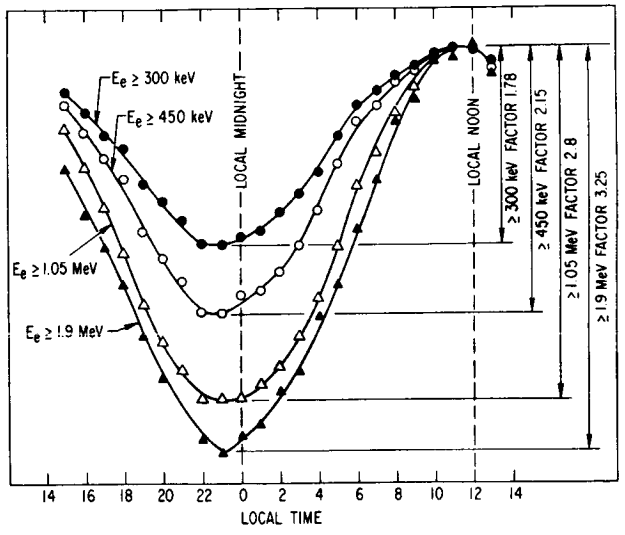


FIGURE 11. -- The diurnal variation of electrons E ≥ 300 keV, ≥ 450 keV, ≥ 1.05 MeV, and ≥ 1.9 MeV at synchronous orbit altitude as measured by ATS-1. The mean of the logarithm of the variation is plotted as a function of local time. (From ref. 14).

The mean of the logarithm of the variation of the fluxes with respect to the flux value at local noon is plotted as a function of local time. The variation is greater for higher energy electrons, which is what one would expect since these L values are near the boundary of stable trapping and the higher energy electrons, which have a larger gyroradius, are more likely to encounter destabilizing conditions near that boundary as they drift in longitude. As an example of how close the boundary is, we can exhibit Figure 12. Two electron flux channels are plotted along with a magnetometer output. The

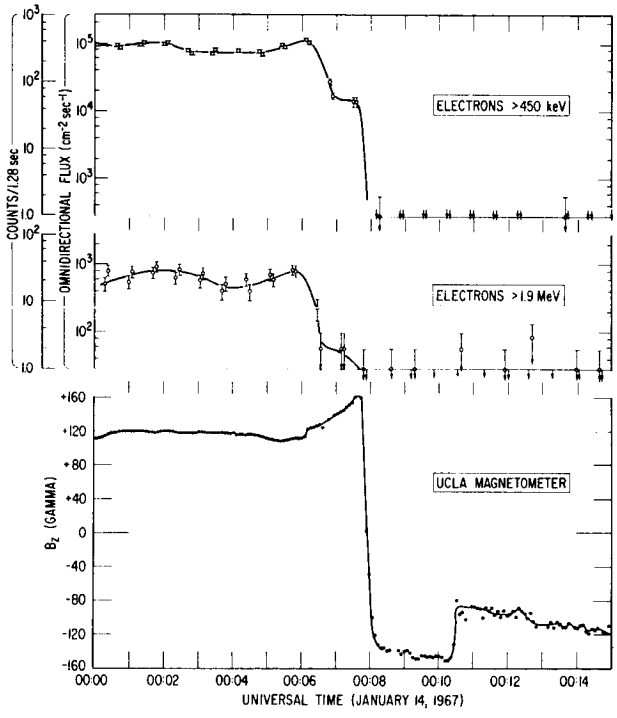


FIGURE 12. -- ATS-1 particle and magnetometer data showing an event in which the magnetospheric boundary moved inside the orbit of the spacecraft. (From ref. 15.)

The effects of magnetic activity on the flux intensities can be seen in Figure 13. Fluxes of electrons with E > 1.05 MeV and E > 1.9 MeV are shown for the time period day 340, 1966 to day 60, 1968 along with the magnetic activity index $\Sigma K_p$. The correlation between increases in magnetic activity and flux increases is quite evident. Changes of flux intensity of an order of magnitude in tens of minutes are observed on plots with shorter time scales. A comparison of the ATS-1 data with the AE3 electron environment (ref. 12) has been made and is shown in Figure 14 (from ref. 14). The AE3 prediction of the probability (P) that a flux (F) greater than a given flux ($F_x$) will be observed is plotted as a function of $F_x$ for several energies. The actual observations by the ATS-1 instrumentation are also shown. The agreement is excellent except at the highest energy. The AE3 environment was compiled from data obtained during and just after a minimum in solar activity. We have seen in the first section that the outer zone energetic electron population responds to magnetic activity which, in turn, is controlled by solar activity. The ATS-1 data was gathered during the rising portion of a solar cycle just prior to the peak. Hence we would expect the ATS-1 energetic particle data to exceed the AE3 predictions, as it does.

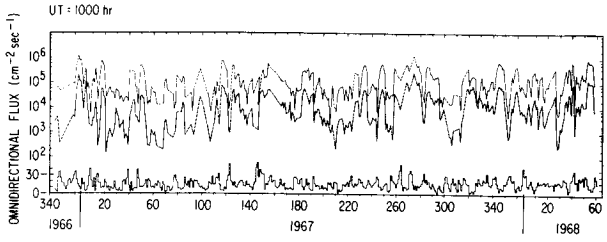


FIGURE 13. -- Flux of electrons E ≥ 1.05 MeV (upper trace) and ≥ 1.9 MeV (lower trace) for the time interval day 340, 1966 to day 60, 1968 at a local time of midnight. The daily sum of the magnetic activity index $K_p$ is plotted at the bottom of the figure. (From ref. 14.)

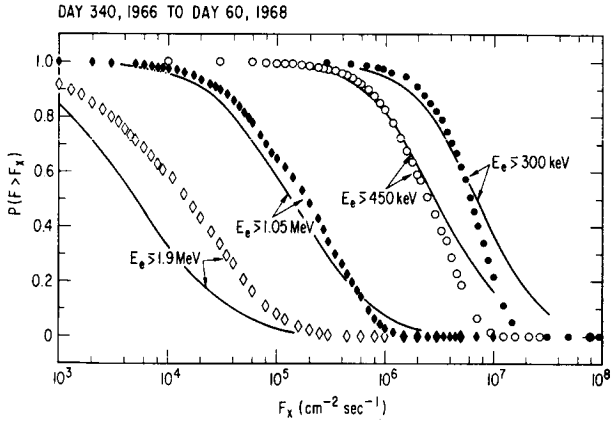


FIGURE 14. -- A comparison between electron fluxes predicted by the AE3 synchronous altitude model environment (ref. 2) and ATS-1 measured values. P(F > $F_x$) is the probability of observing a flux F greater than a given flux $F_x$. The agreement is excellent except for the highest energy electrons. (From ref. 14.)

## REFERENCES


1. Vette, J. I.; Lucero, A. B. and Wright, J. A., Models of the Trapped Radiation Environment, Volume II: Inner and Outer Zone Electrons, NASA Document NASA SP-3024, 1966.
2. Vette, J. I. and Lucero, A. B., Models of the Trapped Radiation Environment, Volume III: Electrons at Synchronous Altitudes, NASA Document NASA SP-3024, 1967.
3. Frank, L. A., J. Geophys. Res., Vol. 70, 1965, p. 1593.
4. Frank, L. A., J. Geophys. Res., Vol. 70, 1965, p. 3533.
5. Williams, D. J.; Arens, J. F. and Lanzerotti. L. J., J. Geophys. Res., Vol. 73, 1968, p. 5673.
6. McIlwain, C. E., J. Geophys. Res., Vol. 66, 1961, p. 3691.
7. Vampola, A. L., Recent Measurements of Inner Zone Electron Lifetimes, COSPAR, London, 1967.
8. Freden, S. C.; Blake, J. B. and Paulikas, G. A., Earth's Particles and Fields (ed. by B. M. McCormac), Reinhold Books Corporation, New York, 1967, p. 3.
9. Pfitzer, K. A. and Winckler, J. R., J. Geophys. Rev., Vol. 73, 1968, p. 5792.
10. Vampola, A. L., Trans, Am. Geophys. Union, Vol. 49, 1968, p. 719.
11. Armstrong, J. C. and Bostrom, C. O., Trans. Am. Geophys. Union, Vol. 51, 1970, p. 393.
12. Mihalov, J. D. and White, R. S., J. Geophys. Res., Vol. 71, 1966, p. 2217.
13. Bostrom, C. O.; Beall, D. S. and Armstrong, J. C., J. Geophys. Rev. Vol. 75, 1970, p. 1246.
14. Paulikas, G. A.; Blake, J. B. and Palmer, J. A., Energetic Electrons at the Synchronous Altitude: A Compilation of Data, The Aerospace Corporation Report TR-0066(5260-20)-4, 1969.
15. Paulikas, G. A.; Blake, J. B.; Freden, S. C.; and Imamoto, S. S.; J. Geophys. Res., Vol. 73, 1968, p. 5743.